

# Chain Formation by Spin Pentamers in $\eta\text{-Na}_9\text{V}_{14}\text{O}_{35}$

D. V. ZAKHAROV<sup>1</sup>, H.-A. KRUG VON NIDDA<sup>1</sup>, J. DEISENHOFER<sup>1</sup>, F. SCHRETTLE<sup>1</sup>, G. OBERMEIER<sup>2</sup>, S. HORN<sup>2</sup> and A. LOIDL<sup>1</sup>

<sup>1</sup> *Experimental Physics V, Center for Electronic Correlations and Magnetism, University of Augsburg – Universitätsstraße 2, 86135 Augsburg, Germany*

<sup>2</sup> *Experimentalphysik II, Institut für Physik, Universität Augsburg – Universitätsstraße 2, 86135 Augsburg, Germany*

PACS 76.30.-v – Electron paramagnetic resonance and relaxation

PACS 65.40.Ba – Heat capacity

PACS 75.10.Pq – Spin chain models

**Abstract.** – The nature of the gapped ground state in the quasi-one-dimensional compound  $\eta\text{-Na}_9\text{V}_{14}\text{O}_{35}$  cannot easily be understood, if one takes into account the odd number of spins on each structural element. Combining the results of specific heat, susceptibility and electron spin resonance measurements we show that  $\eta\text{-Na}_9\text{V}_{14}\text{O}_{35}$  exhibits a novel ground state where multi-spin objects build up a linear chain. These objects - pentamers - consist of five antiferromagnetically arranged spins with effective spin 1/2. Their spatial extent results in an exchange constant along the chain direction comparable to the one in the high-temperature state.

**Introduction.** – The complex magnetic properties of transition-metal oxides are a consequence of the strong interplay of charge, spin, lattice, and orbital degrees of freedom [1]. The physics becomes particularly fascinating in systems with lower dimensionality, where quantum fluctuations suppress the conventional magnetic order [2] in favour of exotic ground states like the spin-Peierls dimerization in  $S = 1/2$  chains [3] or the Haldane-gap formation in integer-spin chains [4].

Among all low-dimensional transition-metal oxides one can single out the vanadium bronzes which acquired a paradigmatic status because of the variety of phenomena displayed by these systems. The possibility to tune the vanadium valence between  $\text{V}^{4+}$  ( $3d^1$ ) and  $\text{V}^{5+}$  ( $3d^0$ ) allows the realization of a multitude of spin-1/2 systems with strong quantum effects. Moreover, the rich structural chemistry of these systems, where the V ions can occur in pyramidal, tetrahedral, or octahedral coordination, gives rise to the formation of very interesting chain- and ladder-like structures [5–7]. The quarter-filled spin ladder  $\alpha'\text{-NaV}_2\text{O}_5$  [8,9] and the one-dimensional metal  $\beta\text{-Na}_{1/3}\text{V}_2\text{O}_5$  [10,11] are the most intensively studied members of this series. The former system reveals charge ordering with the opening of a spin gap similar to a spin-Peierls transition, the latter shows a metal-to-insulator transition and even becomes superconducting under pressure.

In this Letter we focus on a vanadium oxide bronze

with higher Na concentration,  $\eta\text{-Na}_9\text{V}_{14}\text{O}_{35}$ . This system came recently into the focus as a unique example of a low-dimensional spin-gap system [12]. The temperature dependence of the susceptibility indicates the opening of a spin gap below 30 K, while at high temperatures following the Bonner-Fisher (BF) law [13] with  $J \simeq 190$  K. Its low-temperature behavior, however, cannot be described by any known model for spin-gap systems [12]. The room-temperature structure of  $\eta\text{-Na}_9\text{V}_{14}\text{O}_{35}$  is monoclinic with space group  $P2_1/c$ . As depicted in Fig. 1 the structure consists of double chains of the corner-sharing  $\text{VO}_4$  pyramids running along the  $a$  direction, exhibiting, however, a crystallographic step at every five  $\text{VO}_5$  unit. The edge-sharing exchange interactions inside these chains can be neglected [15]. The double chains are bridged by  $\text{VO}_4$  tetrahedra, containing the non-magnetic  $\text{V}^{5+}$  ions, in the  $(ac)$ -plane to form the  $\text{V}_2\text{O}_5$  layers which are mediated by the Na ions along the  $b$  axis. These chains excluding the steps are structurally similar to those of  $\alpha'\text{-NaV}_2\text{O}_5$ , but have a larger average vanadium valence. Eight out of ten V ions are tetravalent except for two neighboring V ions on the structural step, which share one electron and, therefore, have an average valence +4.5 at high temperatures.

Based on a spin-dimer analysis it was suggested that the system can be understood in terms of 10-node rings of  $\text{V}_{10}\text{O}_{30}$ , with each ring opening a spin gap [16]. This

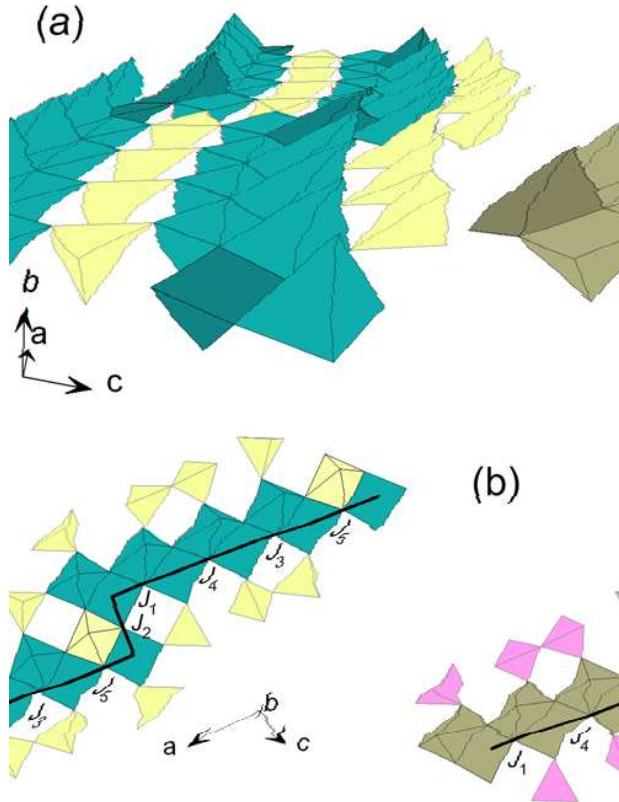


Fig. 1: (color online) (a): Part of the high-temperature ( $T > 100$  K) crystal structure of  $\eta$ - $\text{Na}_9\text{V}_{14}\text{O}_{35}$ . (b): Projection of the low temperature crystal structure onto the  $(ac)$ -plane. The cyan (dark cyan) pyramids correspond to  $\text{V}^{4+}$  ( $\text{V}^{4.5+}$ ) ions surrounded by the  $\text{O}^{2-}$  ions, the light yellow  $\text{VO}_4$  tetrahedra contain non-magnetic  $\text{V}^{5+}$  ions.  $J_i$  denote exchange constants between adjacent V ions along the chain.  $\{a', b', c'\}$  denotes the local coordinate system of the  $\text{VO}_5$  pyramids.

scenario has been discarded by Duc *et al.* [17] arguing that a spin gap can only occur, if the number of magnetic sites per unit cell is even. With its nine magnetic sites per unit cell this is evidently not the case for  $\eta$ - $\text{Na}_9\text{V}_{14}\text{O}_{35}$ . The authors attempted to explain the occurrence of a spin gap with the observed charge ordering superstructure on the two  $\text{V}^{4.5+}$  sites at the structural step below 100 K, which subsequently leads to a larger unit cell doubled along the  $b$ -axis and 18 spins per unit cell. However, the weak exchange coupling between adjacent layers along the  $b$  axis [16] casts doubts upon the effectiveness of such a mechanism for a complete spin-gap formation. Therefore, the inter-chain exchange is thought to be the driving force behind the spin gap opening [17]. Based on a quantitative analysis of all possible exchange paths Koo and Whangbo [15] recently proposed that the magnetic structure of  $\eta$ - $\text{Na}_9\text{V}_{14}\text{O}_{35}$  is build up by chains of 12-spin-rings alternating with chains of 10-spin rings implying the existence of two different spin gaps. Alone, no experimental evidence for such a scenario has been reported and the challenging task remains to consistently describe the

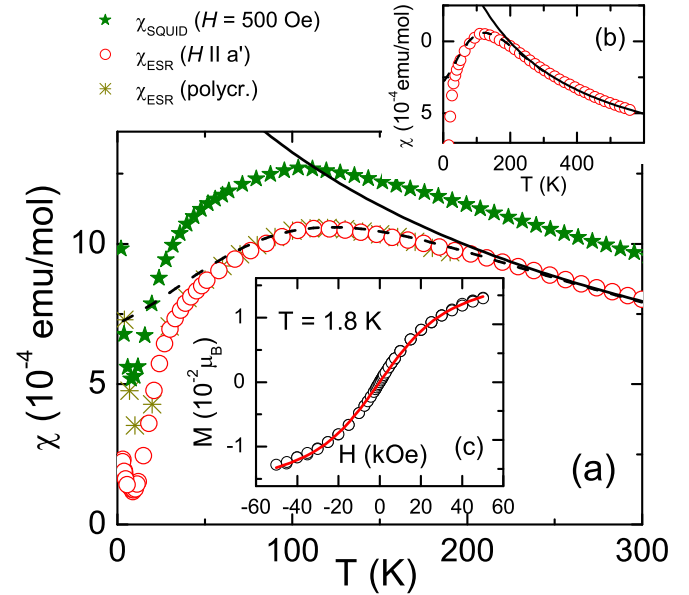


Fig. 2: (color online) Main frame (a): Temperature dependence of the spin susceptibility  $\chi$  measured both by SQUID magnetometry and ESR in  $\text{Na}_9\text{V}_{14}\text{O}_{35}$ . The black dash line represents the prediction of the BF model [13] with  $J/k_B = 190$  K and nine spins on each structural element, the solid line – of the Curie-Weiss model with  $\Theta = -200$  K. The enlarged view of the low-temperature data is presented in Fig. 3. Inset (b): Temperature dependence of  $\chi_{\text{ESR}}$  with  $H \parallel a'$  at high temperatures. Inset (c): Magnetization  $M(H)$  at  $T = 1.8$  K. The line represents a fit by a sum of a Brillouin function and a temperature independent term  $M_0 = \chi_0 H$ .

spin-gap-like nature of the magnetic system with structural elements containing an odd number of spins.

In this work we resolve this ostensible contradiction based on the analysis of the magnetic and thermal properties of  $\eta$ - $\text{Na}_9\text{V}_{14}\text{O}_{35}$ . We interpret the magnetic structure to be dominated by continuous spin chains along the  $a$  axis and as a result the opening of the spin gap at low temperatures remains *incomplete*. Our alternative model for the magnetic ground state, namely a spin chain consisting of spin-pentamer building blocks, allows for a consistent description of the properties of  $\eta$ - $\text{Na}_9\text{V}_{14}\text{O}_{35}$ .

#### Sample preparation and experimental details. –

The single crystals of  $\text{Na}_9\text{V}_{14}\text{O}_{35}$  were grown in a two step process: Firstly, pellets of a nearly stoichiometric mixture of high purity  $\text{NaVO}_3$  and  $\text{VO}_2$  were pressed and heated in an evacuated quartz tube at  $650^\circ\text{C}$  for four days. Then the material was heated above the melting temperature and, in a temperature gradient, was cooled down at a cooling rate of  $7^\circ\text{C}/\text{h}$ . Debye-Scherrer x-ray diffraction and Laue diffraction showed the material to be single phase. The heat-capacity and susceptibility measurements have been performed with a commercial physical properties measurement system (PPMS) and a SQUID magnetometer (MPMS5), both from Quantum Design, for temperatures  $1.8 \text{ K} < T < 300 \text{ K}$ . The Electron Spin Res-

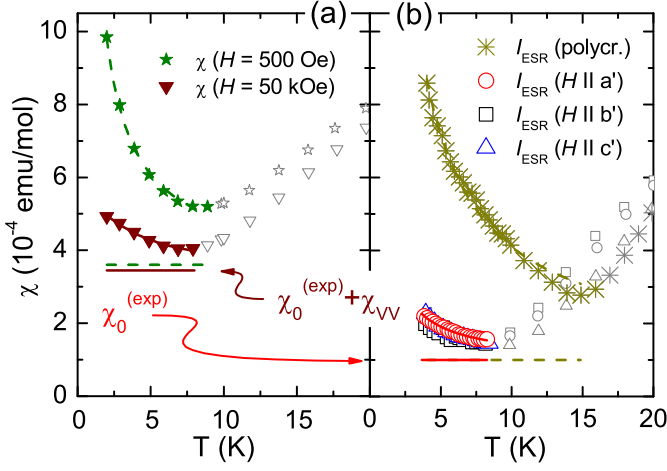


Fig. 3: (color online) Magnetic susceptibility of  $\text{Na}_9\text{V}_{14}\text{O}_{35}$  at low temperatures. The lines represent fits by a sum of a Brillouin function and a temperature independent term  $\chi_0$  (shown separately as a constant contribution). (a): Susceptibility in a polycrystal measured by SQUID magnetometry in a magnetic field  $H = 500$  Oe (green stars) and  $H = 50$  kOe (dark-red triangles). (b): Intensity of the ESR signal  $I_{\text{ESR}}$  in a polycrystal (dark-yellow cross stars) and in a single crystal for the magnetic field applied along the three crystallographic axes.

onance (ESR) experiments have been carried out with a Bruker ELEXSYS E500 CW-spectrometer at X-band frequency ( $\nu \approx 9.4$  GHz). The details of the experimental ESR set-up can be found elsewhere [18]. The obtained ESR spectra are in good agreement with previously published results [17]. For the heat-capacity measurements polycrystalline samples with appropriate mass were used.

**Magnetic Susceptibility.** – We will start with the analysis of the spin susceptibility of the system as measured by ESR. To calculate the absolute values of the spin susceptibility  $\chi_{\text{ESR}}$  in  $\eta$ - $\text{Na}_9\text{V}_{14}\text{O}_{35}$  from the double-integrated ESR spectra, we compared the measured intensities to the ESR signal of the reference compound  $\text{Gd}_2\text{BaCuO}_5$ . The  $dc$ -susceptibility of this system follows a Curie-Weiss law  $\chi_{\text{ESR}} = C/(T - \Theta)$  at  $T > 100$  K, the Curie constant of which corresponds to the contribution of all Gd ions [19]. For this comparison we used the high-temperature ESR data (for  $T > 300$  K) of  $\text{Na}_9\text{V}_{14}\text{O}_{35}$  which can be described by a Curie-Weiss law with  $\Theta = -200$  K (see Fig. 2(b)).

The obtained effective magnetic moment  $\mu_{\text{eff}} = 5 \mu_{\text{B}}$  coincides well with the magnetic moment  $\mu_{\text{theor}} = 5.1 \mu_{\text{B}}$  expected for nine magnetic  $\text{V}^{4+}(3d^1)$  ions per unit cell. Therefore, we conclude that all vanadium ions participate in the generation of the ESR signal in  $\text{Na}_9\text{V}_{14}\text{O}_{35}$ .

Fig. 2 shows the temperature dependence of  $\chi_{\text{ESR}}$  measured both in a single crystal (with  $H \parallel a'$ ) and in a polycrystalline sample. Below room temperature  $\chi_{\text{ESR}}$  does not follow the Curie-Weiss law anymore. Such kind of behavior is typical for one-dimensional spin systems and

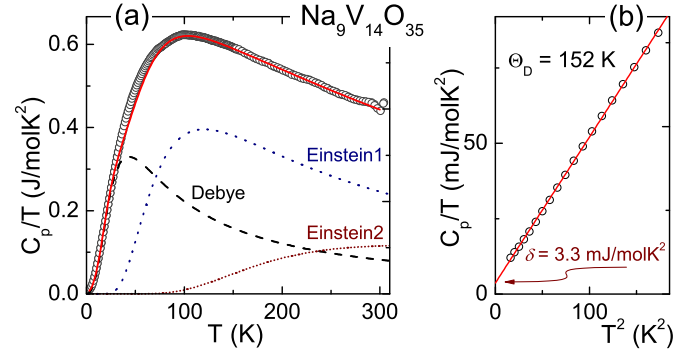


Fig. 4: (color online) (a): Heat capacity of  $\eta$ - $\text{Na}_9\text{V}_{14}\text{O}_{35}$  plotted as  $C_p/T$  vs  $T$ . The contribution of acoustical Debye-phonons is indicated by the dashed black line, contributions of two Einstein modes with  $\Theta_{\text{E1}} = 310$  K and  $\Theta_{\text{E2}} = 850$  K by the blue dotted and the wine short-dotted line, respectively. The sum of all contributions (red solid line) represents the best fit to the experimental results. Frame (b) emphasizes the Debye and the spin-chain contribution at low temperatures.

can be fitted by using the Bonner-Fisher (BF) model [13]. Using the integral of the isotropic exchange between neighboring spins  $J/k_{\text{B}} \approx 190$  K and assuming nine spins per unit cell, we were able to describe the magnitude and the temperature dependence of the susceptibility down to  $T \sim 50$  K.

Let us now compare the spin susceptibility obtained from the intensity of the ESR absorption signal  $\chi_{\text{ESR}}$  with the magnetic  $dc$ -susceptibility  $\chi_{\text{SQUID}}$  measured by SQUID magnetometry. As one can see in Fig. 2, both of them have the same temperature dependence with a broad maximum at around 100 K, in accordance with Refs. [12, 17]. The  $dc$ -susceptibility is larger because of the Van Vleck (VV) orbital contributions to the static susceptibility, which do not affect the spin susceptibility measured by ESR [14].

Below 50 K the data decrease faster than the BF law suggesting a dimerization of the spins, but finally turn up again below 15 K. Such an increase of the susceptibility to lower temperatures usually arises owing to a small amount of paramagnetic impurities present in the samples. The measurements of the magnetization  $M(H)$  (Fig. 2(c)) and of the susceptibility in a higher field  $H = 50$  kOe (Fig. 3(a)) show that this paramagnetic contribution starts to saturate already above  $H \approx 10$  kOe. The fit curves given in the pictures represent the best fit of these data achieved by a sum of a Brillouin function

$$M \propto (2S + 1) \text{cth} \left( \frac{2S + 1}{2S} \frac{\gamma S H}{k_{\text{B}} T} \right) - \text{cth} \left( \frac{1}{2S} \frac{\gamma S H}{k_{\text{B}} T} \right) \quad (1)$$

( $\gamma$  denote the gyromagnetic ratio,  $k_{\text{B}}$  is the Boltzmann constant, the spin  $S = 1/2$ ) and a temperature independent contribution  $M_0 = \chi_0 H$ . An alternative description of the low-temperature susceptibility with a Curie-Weiss law taking into account a residual magnetic interaction

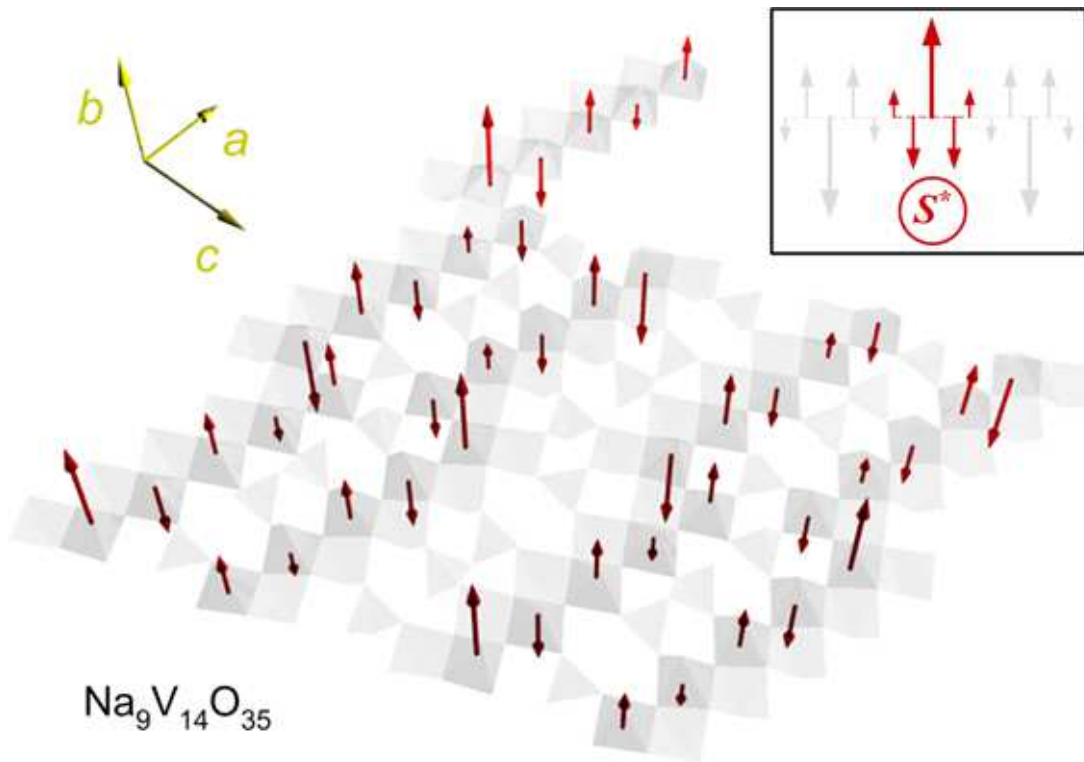


Fig. 5: (color online) Schematic spin structure of the proposed ground state in  $\eta\text{-Na}_9\text{V}_{14}\text{O}_{35}$  at  $T < 10$  K. The inset shows the spin structure which appears near an unpaired spin. The arrows represent the average spin projections at the lattice sites.

felt by impurities but without any constant contribution was proposed in Ref. [17]. This allowed to fit  $\chi(T)$  at low fields only, but we did not achieve a reasonable description of the field dependence of the magnetization and of the high-field susceptibility in terms of this approach.

The Brillouin contribution is a sign of free impurity spins, while the temperature independent susceptibility  $\chi_0$  may, in principle, originate from four possible contributions, namely, (i) saturated ferromagnetic moments, (ii) Pauli paramagnetism, (iii) the Van Vleck orbital paramagnetism, and (iv) the spin chain contribution: The paramagnetic behavior of the magnetization  $M(H)$  (Fig. 2(c)) allows to exclude the presence of ferromagnetic moments in the sample. To check for Pauli paramagnetism we performed dielectric measurements of  $\eta\text{-Na}_9\text{V}_{14}\text{O}_{35}$  that revealed values of the electric conductivity less than  $10^{-12} \Omega^{-1}\text{cm}^{-1}$  for  $T < 50$  K and, hence, allow to neglect a possible electronic contribution to  $\chi_0$ . The magnitude of the Van Vleck term  $\chi_{\text{VV}}$  can be estimated by comparison with ESR data, because the intensity of the ESR absorption signal  $\chi_{\text{ESR}}$  is not sensitive to VV contributions. As one can see in Fig. 3(b) the temperature independent background is indeed considerably smaller for  $\chi_{\text{ESR}}(T)$ , but still remarkable and amounts to  $\chi_0^{(\text{exp})} \approx 0.95 \cdot 10^{-4}$  emu/mol [20]. Consequently, we find ourselves left with the contribution of a spin-chain system which seems to survive despite the considerable reduction

of the susceptibility at  $T \sim 30$  K.

To resolve this challenging task we start out with the analysis of the spin chain contribution to the magnetic and thermodynamic properties in the low-temperature phase: According to Bonner and Fisher [13], the magnitude of the susceptibility at zero temperature  $\chi_0^{(\text{BF})}$  is expected to be about 0.69 of its maximal value  $\chi_{\text{max}}^{(\text{BF})} = 0.147 \cdot g^2 \mu_{\text{B}}^2 N / |J|$ . Using  $\chi_{\text{max}} \approx 10.6 \cdot 10^{-4}$  emu/mol (Fig. 2), one gets  $\chi_0^{(\text{BF})} \approx 7.3 \cdot 10^{-4}$  emu/mol. The experimental contribution  $\chi_0^{(\text{exp})}$ , however, amounts to 13% of this value only.

Let us turn now to the results of the specific heat measurements which confirm the presence of the spin chain contribution at low temperatures in  $\eta\text{-Na}_9\text{V}_{14}\text{O}_{35}$ . Moreover, the magnitude of this contribution turns out to be in good agreement with the susceptibility data.

**Specific Heat.** – Following Bonner and Fisher [13] a linear increase  $C_{\text{p}}(T) = \delta T$  of the specific heat is characteristic for a linear antiferromagnetic spin-1/2 chain at low temperatures  $T \ll |J|/k_{\text{B}}$ . The plot of  $C_{\text{p}}/T$  vs.  $T^2$  allows to reveal this type of behavior and estimate the magnitude of  $\delta$ . Fig. 4(b) shows that the specific heat of  $\text{Na}_9\text{V}_{14}\text{O}_{35}$  at low temperatures  $T < 5$  K cannot be explained by the Debye-contribution  $C_{\text{p}}(T \ll \Theta_{\text{D}}) \propto T^3$  only. Because of the underlying linear contribution the fit line crosses the ordinate axis not in the origin but

at  $C_p/T = \delta_{\text{exp}} = 3.3 \text{ mJ/molK}^2$ . This value is again smaller than the expected one and amounts to approximately 11.3% of the value predicted by the calculations of Bonner and Fisher  $\delta_{\text{BF}} = 0.7k_{\text{B}}R/|J| \approx 29.1 \text{ mJ/molK}^2$ .

To summarize the experimental findings so far, both the magnetic and the thermodynamic properties of a linear spin-1/2 chain are present in  $\text{Na}_9\text{V}_{14}\text{O}_{35}$  despite the partial dimerization of the spin structure at  $T < 50 \text{ K}$ . Only the corresponding parameters  $\chi_0$  and  $\delta$  are modified pointing at a nontrivial distribution of the spin density and the exchange coupling constants along the chain. In the following we will try to reproduce the low-temperature spin structure based on the previous results [15, 17], our experimental data, and the theoretical calculations [13].

**Analysis.** – The origin of the spin-chain contributions becomes clear, if one takes into account the results of the spin-dimer analysis by Koo and Whangbo [15]. According to them, the high-temperature  $T > 100 \text{ K}$  magnetic structure can be considered as a quasi-one-dimensional system consisting of double chains running along the  $a$  direction (see Fig. 1(a)). At low temperatures one of the adjacent chains breaks off, whereas the second one  $(J_5 - J_3 - J_4 - J_1 - J_2)_{\infty}$ , shown by the black line in Fig. 1(b), survives with almost unchanged exchange parameters  $J_i$  along the chain. This chain can be regarded as a result of linking pentamers with the  $J_3 - J_4 - J_1 - J_2$  paths through the paths  $J_5$  [15]. The spin pentamer does not have a spin gap preserving the spin-chain properties down to lower temperatures. Two of these properties, a temperature independent contribution to the magnetic susceptibility and a linear contribution to the specific heat, are clearly seen in the experiment.

The magnitude of these contributions in the low-temperature phase can be estimated using the following expressions [13]:

$$\chi_0 = \frac{g^2 \mu_{\text{B}}^2}{\pi^2} \cdot \left(\frac{N}{J}\right), \quad \delta = 0.7 k_{\text{B}}^2 \cdot \left(\frac{N}{J}\right), \quad (2)$$

where  $N$  and  $J$  denote the number of involved spins and the effective exchange integral, respectively. The values of these contributions,  $\chi_0^{(\text{BF})}$  and  $\delta_{\text{BF}}$ , estimated previously, were obtained using the high-temperature values of  $N$  (nine spins per structural element) and  $J$  (190 K). Whereas the values of exchange integrals along the chain remain almost unaffected by the charge-ordering transition at  $T \approx 100 \text{ K}$  [15], the number of involved spins  $N$  might be changed at lower temperatures and be responsible for the reduced magnitude of these contributions  $\chi_0^{(\text{exp})}$  and  $\delta_{\text{exp}}$ .

All models of the low temperature magnetic ground state proposed so far [15, 17] cannot explain the presence and the magnitude of  $\chi_0^{(\text{exp})}$  and  $\delta_{\text{exp}}$ . However, it can be understood on the basis of an effect predicted theoretically [22] in the diamagnetically diluted spin-Peierls system  $\text{CuGeO}_3$  and confirmed experimentally in

$\text{Cu}_{1-x}\text{Mg}_x\text{GeO}_3$  [23] and  $\text{Pb}(\text{Ni}_{1-x}\text{Mg}_x)_2\text{V}_2\text{O}_8$  [24]. In these works it was shown that an impurity spin causes the occurrence of a local magnetization on the neighboring sites in order to gain exchange energy. The induced magnetic moment is staggered because of the antiferromagnetic coupling between the spins and decreases with increasing distance from the impurity spin as shown schematically in the inset of Fig. 5. However, the net magnetic moment of the whole structure remains equal to  $1\mu_{\text{B}}$ . The characteristic length  $L$  of this multi-spin object (the extension of short range antiferromagnetic ordering) along the chain direction depends on temperature  $J S^2 e^{-2L/\xi} \sim k_{\text{B}}T$  and is of the order of the correlation length  $\xi$ , which was estimated to be of about ten interspin distances for the above compounds.

In  $\eta$ - $\text{Na}_9\text{V}_{14}\text{O}_{35}$  each structural pentamer (five V ions connected via  $J_3 - J_4 - J_1 - J_2$ , see Fig. 1) possesses an odd number of spins. Hence, one of them (every fifth one) is uncompensated and serves as an impurity spin  $S^* = 1/2$ . By analogy with the cases described in Refs. [22–24], this magnetic moment will spread out on the neighboring four spins building spin pentamers, objects with five antiferromagnetically coupled spins with effective spin 1/2 (see the inset of Fig. 5). Note that these pentamers overlap strongly because the characteristic magnetic correlation length is of the order of the segment length. Therefore, the spin pentamers has to be coherent along the whole chain (Fig. 5). The magnetic and thermal properties of this effectively antiferromagnetic chain consisting of such spin pentamers are expected to be quantitatively different from the original chain because of the considerably smaller average magnetic moment on each site. But the exchange energy of this structure with an almost unchanged local exchange constant can still produce a linear contribution to the specific heat and a temperature independent contribution to the susceptibility. The experimental results evidence the presence of these contributions.

The values of these contributions are supposed to be nine times smaller as compared to the values expected for two non-dimerized  $S = 1/2$  chains (with 9 spins per 10 sites) realized at high-temperatures: one of the chains is completely broken off at low temperatures and the effective spin of the second chain becomes five times smaller. The experimental reduction factors 0.13 for the susceptibility and 0.113 for the specific heat are in good accordance with the expected ratio  $1/9 \approx 0.111$ .

Thus, the spin-gap opening in the low-temperature state of  $\eta$ - $\text{Na}_9\text{V}_{14}\text{O}_{35}$  turns out to be incomplete. This conclusion is supported by a recent polarized Raman-scattering investigation [25]. The observed Raman modes become narrower, change their energy and width, but no new modes were detected on lowering the temperature down to 10 K, although it is natural to expect the appearance of new modes in the spin or phonon channel in case of a conventional charge ordering transition with doubling of the  $b$  axis [17]. The small intensity of that scattering might be due to the residual dynamical spin-chain structure ex-

isting down to lowest temperatures. Moreover, the proposed spin-pentamer state successfully explains the puzzling controversy between the originally suggested singlet ground state and the odd number of spins per unit cell in the structure. Note that in the case observed in doped spin-Peierls and Haldane chains [23, 24], these multi-spin objects are diluted and randomly distributed in the lattice. That gives rise to impurity induced local magnetic order and phase separation. In contrast,  $\eta$ - $\text{Na}_9\text{V}_{14}\text{O}_{35}$  provides a regular lattice of such spin objects leading the formation of a new exotic ground state.

**Summary.** — In summary, a model for the magnetic ground state in the quasi-one dimensional spin system  $\eta$ - $\text{Na}_9\text{V}_{14}\text{O}_{35}$  was proposed. We conclude that the dimerization of spins is far from complete for  $T < 10$  K, and the uncompensated vanadium spins provide a constant contribution to the susceptibility and a linear contribution to the specific heat. The ground state of  $\eta$ - $\text{Na}_9\text{V}_{14}\text{O}_{35}$  can be understood in terms of "spin pentamers" as building units of a linear chain along the crystallographic  $a$  axis.

\* \* \*

We thank C. Helbig, P. Lunkenheimer and J. Hemberger for useful discussions. This work was supported by the DFG within SFB 484 (Augsburg) and by the Volkswagen-Stiftung.

## REFERENCES

- [1] Y. IMADA, A. FUJIMORI and Y. TOKURA, *Rev. Mod. Phys.*, **70** (1998) 1039.
- [2] N. D. MERMIN and H. WAGNER, *Phys. Rev. Lett.*, **17** (1966) 1133.
- [3] E. PYTTE, *Phys. Rev. B*, **10** (1974) 4637.
- [4] F. D. M. HALDANE, *Phys. Rev. Lett.*, **50** (1983) 1153.
- [5] H. T. EVANS JR. and J. M. HUGHES, *Amer. Miner.*, **75** (1990) 508.
- [6] Y. KANKE, K. KATO, E. TAKAYAMA-MUROMACHI and Y. MATSUI, *J. Solid State Chem.*, **89** (1990) 130.
- [7] V. A. IVANSHIN, V. YUSHANKHAI, J. SICHELSCHMIDT, D. V. ZAKHAROV, E. E. KAUL and C. GEIBEL, *Phys. Rev. B*, **68** (2003) 064404; *J. Magn. Magn. Mat.*, **272** (2004) 960.
- [8] M. ISOBE and Y. UEDA, *J. Phys. Soc. Jpn.*, **65** (1996) 1178.
- [9] M. V. EREMIN, D. V. ZAKHAROV, R. M. EREMINA, J. DEISENHOFER, H.-A. KRUG VON NIDDA, G. OBERMEIER, S. HORN and A. LOIDL, *Phys. Rev. Lett.*, **96** (2006) 027206.
- [10] H. YAMADA and Y. UEDA, *J. Phys. Soc. Jpn.*, **68** (1999) 2735.
- [11] M. HEINRICH, H. A. KRUG VON NIDDA, R. M. EREMINA, A. LOIDL, CH. HELBIG, G. OBERMEIER and S. HORN, *Phys. Rev. Lett.*, **93** (2004) 116402.
- [12] M. ISOBE, Y. UEDA, Y. OKA and T. YAO, *J. Solid State Chem.*, **145** (1999) 361.
- [13] J. C. BONNER and M. E. FISHER, *Phys. Rev.*, **135** (1964) A640.
- [14] K. YOSIDA, *Theory of Magnetism*, edited by P. FULDE (Springer, Heidelberg) 1996, p. 36.
- [15] H.-J. KOO and M.-H. WHANGBO, *Solid State Comm.*, **9** (2007) 824.
- [16] M.-H. WHANGBO and H.-J. KOO, *J. Solid State Comm.*, **115** (2000) 115.
- [17] F. DUC, P. MILLET, S. RAVY, A. THIOU, F. CHABRE, A. M. GHORAYEB, F. MILA and A. STEPANOV, *Phys. Rev. B*, **69** (2004) 094102.
- [18] D. V. ZAKHAROV, J. DEISENHOFER, H.-A. KRUG VON NIDDA, P. LUNKENHEIMER, J. HEMBERGER, M. HOINKIS, M. KLEMM, M. SING, R. CLAESSEN, M. V. EREMIN, S. HORN and A. LOIDL, *Phys. Rev. B*, **73** (2006) 094452.
- [19] G. F. GOYA, R. C. MERCADER, L. B. STEREN, R. D. SÁNCHEZ, M. T. CAUSA and M. TOVAR, *J. Phys.: Condens. Matter*, **8** (1996) 4529.
- [20] All quantities refer to one mole of  $\text{Na}_{9/7}\text{V}_2\text{O}_5$ .
- [21] S. A. GOLUBCHIK, M. ISOBE, A. N. IVLEV, B. N. MAVRIN, M. N. POPOVA, A. B. SUSHKOV, Y. UEDA and A. N. VASIL'EV, *J. Phys. Soc. Jpn.*, **66** (1997) 4042.
- [22] H. FUKUYAMA, T. TANIMOTO and M. SAITO, *J. Phys. Soc. Jpn.*, **65** (1996) 1182.
- [23] V. N. GLAZKOV AND A. I. SMIRNOV, H.-A. KRUG VON NIDDA, A. LOIDL, K. UCHINOKURA and T. MASUDA, *Phys. Rev. Lett.*, **94** (2005) 057205.
- [24] A. I. SMIRNOV, V. N. GLAZKOV, H.-A. KRUG VON NIDDA, A. LOIDL, L. N. DEMIANETS and A. YA. SHAPIRO, *Phys. Rev. B*, **65** (2002) 174422.
- [25] Z.V. POPOVIC, V.V. MOSHCHALOV, M. ISOBE and Y. UEDA, *Solid State Comm.*, **142** (2007) 385.